A&A 378, 522–538 (2001)
DOI: 10.1051/0004-6361:20011184

Astronomy & Astrophysics

Monitoring of long term behaviour of OH masers in semiregular variables: R Crt, W Hya and RT Vir*

S. Etoka[1,2,**], L. Błaszkiewicz[1], M. Szymczak[1], and A. M. Le Squeren[3]

[1] Toruń Centre for Astronomy, Nicolaus Copernicus University, Gagarina 11, 87100 Toruń, Poland
[2] ARPEGES, Observatoire de Paris, 92195 Meudon, France
[3] GRAAL, Université de Montpellier II, 34095 Montpellier, France

Received 25 June 2001 / Accepted 8 August 2001

Abstract. We present and interpret the results of a long-term OH variability study of three semiregular stars, one type a (SRa), W Hya, and two type b (SRb), R Crt and RT Vir. The 1665 and 1667 MHz OH masers of the three semiregulars were observed at intervals in the period 1982 January–1995 December using the Nançay radio telescope, and we searched for 1612 MHz emission. The OH maser profiles of the studied stars significantly deviated from a standard double-peaked profile. The timescale of profile changes in the two SRb stars R Crt and RT Vir was as short as a month. The OH profiles of the SRa star W Hya were much more stable but since November 1986 a very blue-shifted feature appeared at 1667 MHz. Our phase-lag measurements suggest that this feature comes from a detached OH shell of radius $\sim 3 \times 10^{16}$ cm. Faint 1612 MHz emission was found in W Hya only. Weak emission at velocities very close to the systemic velocity usually appeared during some intervals of high maser activity in R Crt and RT Vir and was almost always present in W Hya. For R Crt we estimated that this tangential emission disappeared when the kinetic temperature in the OH maser regions dropped below 150−200 K. For a few features, line narrowing and re-broadening were observed on timescales of 90−200 days. The linewidth was inversely proportional to the peak flux density, suggesting unsaturated amplification. Cyclic variations in the integrated flux density were observed in all the three stars. The OH variability curves were generally characterised by large amplitude ($4-6^{\rm m}$) variations over 400−800 days superimposed with 100−300-day variations of $0.2-2^{\rm m}$. Only the measured OH period of W Hya, of 362 ± 7 days, was in agreement with the optical period. The two SRb stars exhibited multi-periodic OH variability including with two statistically significant periods. The behaviour of their red- and blue-shifted emission was less correlated than in W Hya. The ratios of the flux densities at 1667 MHz to that at 1665 MHz in all the three stars were about 2 at epochs of high OH activity and usually increased during weak maser emission. Long term behaviour of the OH masers from W Hya resembled that of standard OH Miras, while that of R Crt and RT Vir suggested thin and clumpy envelopes where unsaturated emission was sustained in some clouds.

Key words. masers − stars: variable − stars: AGB and post-AGB − circumstellar matter − stars: individual: R Crt − RT Vir − W Hya

1. Introduction

Temporal variability is one of the characteristic properties of circumstellar OH masers. Early observations of Miras and OH/IR objects showed that OH maser emission follows the optical and infrared emission (Harvey et al. 1974; Fillit et al. 1977; Jewell et al. 1979). They show evidence for radiative coupling of the OH maser with stellar variability. Long term studies of Miras spanning about 15 years (Etoka 1996; Etoka & Le Squeren 2000) revealed that the integrated OH flux densities show cyclic variations superimposed on slow changes lasting several stellar cycles. There are some Mira variables which experienced eruptive variability in the OH lines (Jewell et al. 1979; Le Squeren & Sivagnanam 1985; Etoka & Le Squeren 1996; 1997).

In contrast to the extensively studied Mira variables, little is known about the OH variability of semiregular variables (SRs). It is commonly accepted that both classes

Send offprint requests to: M. Szymczak,
e-mail: msz@astro.uni.torun.pl

* Figures A1–A3 are only available in electronic form at http://www.edpsciences.org

** *Present address*: Jodrell Bank Observatory, University of Manchester, Jodrell Bank, Macclesfield, Cheshire SK11 9DL, UK.

of red giants are closely related; their periods are similar, but by definition the light curves of SRs are less regular than that of Miras and their optical amplitudes are less than $2\overset{\mathrm{m}}{.}5$ (Kholopov et al. 1985). The deduced mass loss rate of SRs are lower than that of Miras. An SRs−Miras evolutionary sequence was argued (Kerschbaum & Hron 1992). Young et al. (1993) suggested that some SRs had higher mass loss rates in the past implying that an opposite evolutionary sequence is allowed. The SRs associated with OH maser emission only form a small group; in the close solar neighbourhood about 10% of SRs show OH masers (Szymczak et al. 1995). Furthermore, the OH luminosity and the efficiency of OH pumping by the infrared emission in these stars are lower than those measured in giant stars with higher mass loss rates. The OH maser envelopes of the SRs are usually smaller and thinner than those observed in Miras and OH/IR stars (Szymczak et al. 1998, 1999). Those properties suggest that SRs can be good candidates to search for peculiar and/or non-cyclic variations in the OH maser flux density. A search for such behaviour of OH masers over several stellar cycles in three semiregular variables: R Crt, W Hya and RT Vir is one of the goals of our observations. We report the results of a monitoring program spanning 10−14 years, which duration is comparable to the gas travel time across the OH maser shells of the studied objects.

The observed intensity of OH maser sources can vary due to changes in the pump rate (Harvey et al. 1974; Le Squeren & Sivagnanam 1985) but changes within the maser regions due to shocks or disturbances propagating through the masing column may also be possible causes. OH monitoring data of SRs can provide new evidence which may be useful to verify the recent models of OH variations (Palen & Fix 2000) and OH mainline pumping (Collison & Nedoluha 1993). These monitorings also provide information to supplement high angular resolution images showing the spatial structure of the maser emission (Szymczak et al. 1998, 1999) and help us to understand better the dynamic properties of circumstellar outflow in OH maser envelopes.

2. Observations

Observations were made with the Nançay radio telescope. The half-power beamwidth at 1.6 GHz was $3.5'$ in α by $18'$ in δ. A cooled dual channel receiver was used to obtain signals in left- and right-handed circular polarisations (LHC, RHC) or in two orthogonal linear (horizontal and vertical) polarisations simultaneously. The typical system temperature was about 45 K and the point source sensitivity was $1.1\,\mathrm{Jy\,K^{-1}}$ at 0° declination. The 1024 channel, 7-level digitisation autocorrelation spectrometer was employed, divided into two 512 lag channels or four 256 lag channels providing a velocity resolution of 0.07 or $0.14\,\mathrm{km\,s^{-1}}$, respectively, for both 1665 and 1667 MHz mainlines. Data were acquired in frequency switching mode. Each observation lasted about one hour and a typical 3σ sensitivity was 0.20 Jy for the spectra obtained at $0.14\,\mathrm{km\,s^{-1}}$ of spectral resolution.

Table 1. Expansion (v_e) and systemic (v_s) velocities of the observed SRs

Source	v_e ($\mathrm{km\,s^{-1}}$)		v_s ($\mathrm{km\,s^{-1}}$)	References for v_s
	1665 MHz	1667 MHz		
R Crt	9.2 ± 06	9.2 ± 06	10.2 ± 0.6	1
W Hya	5.5 ± 0.4	6.7 ± 0.4	40.6 ± 0.4	2
RT Vir	6.8 ± 0.4	7.3 ± 0.4	17.5 ± 0.4	1

1. Wallerstein & Dominy (1988); 2. Neufeld et al. (1996).

Monitoring observations of R Crt, W Hya and RT Vir at the 1665 and 1667 MHz in both circular polarisations started in 1982 January, 1986 January and 1982 April, respectively and lasted until 1995 December. We searched for OH 1612 MHz emission towards all the three stars near OH mainline maxima. During the last two years of the monitoring program the targets were also observed in two orthogonal linear polarisations and the results obtained will appear in a separate paper. The flux density scale was established by comparison with observations of W12. It was accurate to within 18% before 1985, about 8% in the period from 1985 to 1993 October and better than 5% since 1993 October. During all the observations, real-time correction was performed for the acceleration of topocentric velocity with respect to the local standard of rest (LSR). The LSR velocity v_LSR was determined with an accuracy better than $0.01\,\mathrm{km\,s^{-1}}$. Through the paper we used the terms red-shifted and blue-shifted to describe the velocity relative to the systemic velocity v_s.

3. Results

3.1. Spectral profiles

The complete atlases of maser spectra of the Stokes parameters I((RHC+LHC)/2) and V((RHC−LHC)/2) of the OH 1667 and 1665 MHz masers of the three sources (Figs. A1–A3) are only available in electronic form.

3.1.1. R Crt

Selected spectra of 1667 and 1665 MHz maser emission from R Crt are shown in Figs. 1 and 2 respectively to illustrate changes in the profile shape. The dates of observations in $\mathrm{JD_m} = \mathrm{JD} - 2\,444\,950$ are added in parentheses. The maximum velocity extent between the extreme peaks observed allows us to estimate the expansion velocity v_e and the systemic velocity (Table 1). In the 1667 and 1665 MHz spectra, three groups of maser features can be distinguished. Two of them, composed of a few blended features, were centred at velocities about 2 and $19\,\mathrm{km\,s^{-1}}$. At some epochs the red-shifted emission fell below our detection threshold. Weak 1667 and 1665 MHz emission sometimes appeared in the central velocity range from 8

to 13 km s^{-1}. The group of red-shifted features centred at $v_{\rm LSR} = 19$ km s^{-1} was strongly circularly polarised in both mainlines and sometimes fully polarised features were observed. Complex spectra in Stokes V were observed for the blue-shifted emission in both mainlines. The circular polarisation of the maser features observed at the central velocities (8−13 km s^{-1}) was usually weak. Our observations revealed no 1612 MHz emission above the 3σ upper limit of 0.20 Jy. A tentative detection of this line in 1971 November was mentioned by Dickinson et al. (1973).

3.1.2. W Hya

A selection of the OH mainline maser profiles from W Hya are shown in Figs. 3 and 4. The 1667 MHz profile had two emission complexes in the velocity ranges 33−38 and 42−48 km s^{-1}, each consisting of 5−9 blended features. Weak emission near 40.4 km s^{-1} sometimes appeared and usually was blended with the red-shifted complex. Extreme blue-shifted emission at 33.8 km s^{-1} was first detected in 1986 November. Values of $v_{\rm e}$ and $v_{\rm s}$ are given in Table 1. The shape of the 1667 MHz spectrum at blue-shifted velocities changed less than that at red-shifted velocities. Significant variations in the Stokes V spectrum was observed at 1667 MHz. The 1665 MHz emission covered the velocity range from 35 to 46 km s^{-1}. Emission was present over almost the entire velocity range. Strong changes in the relative strength of the features were observed within less than two month intervals. Changes in the 1665 MHz profile shape were more prominent than at 1667 MHz. The Stokes V profile had very complicated and variable structure. Observations of W Hya made at 1612 MHz around the OH mainline maxima from 1986 February to 1995 December revealed, in 1992 August, faint polarised emission at $v_{\rm LSR} = 36$ km s^{-1} with the peak fluxes of 0.09 and 0.12 Jy in LHC and RHC, respectively (Fig. 5). 1σ in both polarisations was 0.02 Jy. The velocity of this peak is very close to the velocities of most prominent features at both mainlines.

3.1.3. RT Vir

Figures 6 and 7 show selected OH maser profiles of RT Vir. The 1667 MHz profile had two emission complexes over a velocity range of about 15 km s^{-1}. The blue-shifted complex contained three blended groups of maser features centred near 10.5, 11.3 and 14 km s^{-1} which are sometimes clearly distinct. The red-shifted emission had a velocity extent of 2 km s^{-1}. The 1665 MHz profile strongly deviated from the standard double-peaked profile. Sometimes faint emission appeared at the central velocity of 17.5 km s^{-1} or the blue-shifted emission sharply dropped. The 1665 MHz emission was strongly circularly polarised and more variable than at 1667 MHz. The expansion velocity deduced from the 1665 MHz profile was about 0.5 km s^{-1} lower than that deduced at 1667 MHz (Table 1).

3.2. Average profiles and variability index

The average OH maser profiles for the studied sources are shown in Figs. 8−10. The variability of maser emission for each spectral channel is estimated from the observed variability index $\sigma_{\rm obs}$:

$$\sigma_{\rm obs} = \frac{1}{n}\sum_{i=1}^{n}|S_i - S|, \quad (1)$$

where n is the number of observations, S_i is the flux density at the ith epoch, and S is the mean flux density. The variability index σ (a lower limit to the intrinsic variability index) is then given by $\sigma = \sqrt{\sigma_{\rm obs}^2 - \epsilon^2}$, where ϵ^2 is the mean square error in flux densities. The profile asymmetry is defined as $(S_{\rm pB}/S_{\rm pR})\times 100\%$, where $S_{\rm pB}$ and $S_{\rm pR}$ are the peak flux densities at blue- and red-shifted velocities, respectively.

3.2.1. R Crt

The average maser profiles of R Crt at both transitions were strongly asymmetric; 91% and 84% in peak densities for 1665 and 1667 MHz lines respectively. Both emissions occurred within the same velocity range implying common envelopes (Szymczak et al. 1999). The variability indices generally followed the profile shapes, that is, when S is high then σ is large, which would be expected for a linear amplification of maser emission in a homogeneous envelope.

3.2.2. W Hya

The average 1665 and 1667 MHz profiles of W Hya also showed significant asymmetry of 65% and 85% respectively. The 1667 MHz emission overshoots the 1665 MHz emission by about 1.5 km s^{-1} which can be easily explained by the observational fact that the masers come from different regions (Szymczak et al. 1998). Broad and weak emission near the systemic velocity was present at both frequencies. This suggests tangential amplification in the envelope. The variability index across the profiles generally was proportional to the maser fluxes. At 1667 MHz, however, this index is slightly higher for the red-shifted emission than for the blue-shifted emission of similar average flux density. Considerable increase of σ at a velocity of about 46.5 km s^{-1} suggests that at some epochs this feature was very weak or completely disappeared. Indeed, inspection of Fig. 3a revealed that this emission was present in two intervals; 1992 January − October and 1994 September − 1995 November. Further analysis in Sect. 3.4 shows that it significantly contributes to the integrated flux density. We conclude that at least the extreme red-shifted emission at 1667 MHz experienced eruptive variability.

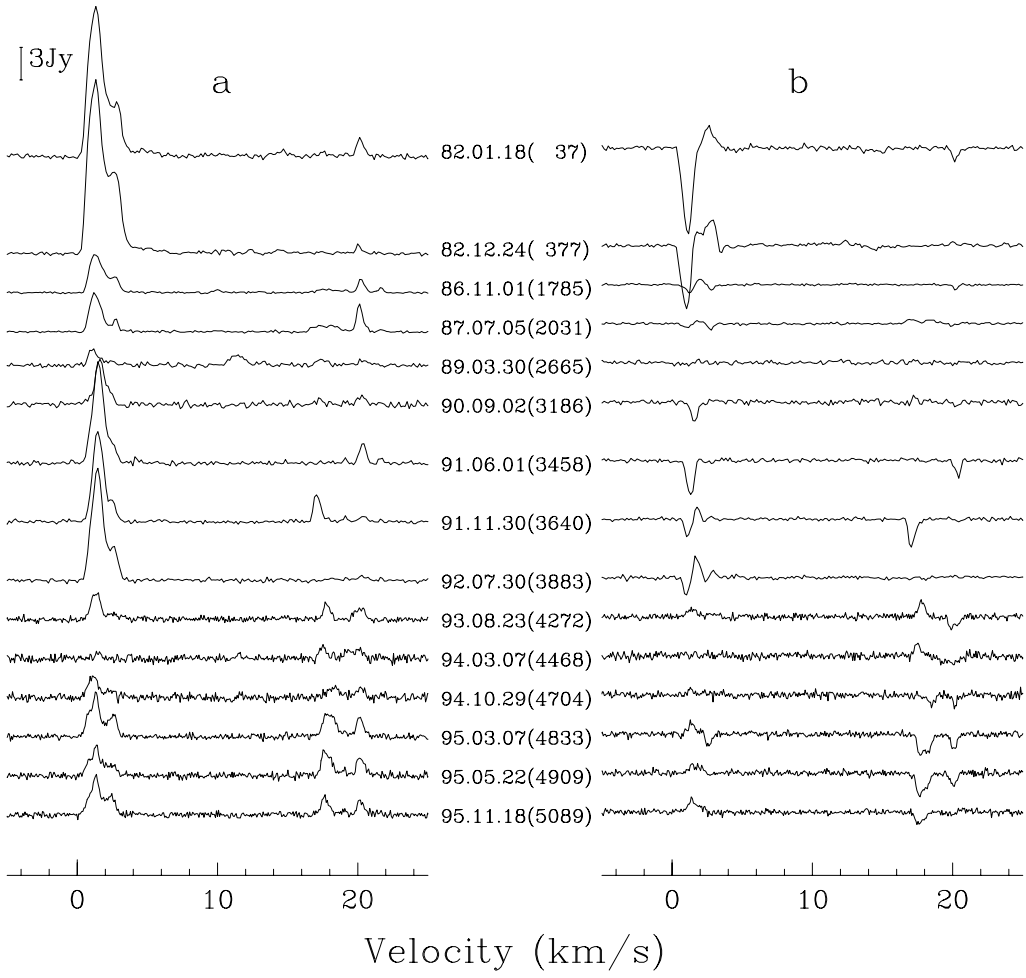

Fig. 1. Selected spectra of the OH 1667 MHz maser emission from R Crt in **a)** Stokes I and **b)** Stokes V taken from 1982 January to 1995 November. The flux density scale is shown by the vertical bar. JD_m dates are given in parentheses.

3.2.3. RT Vir

The average maser profiles of RT Vir were asymmetric (70−50%) and of very different shapes in both transitions. The variability index across the 1667 MHz profile showed very unusual behaviour. There were three features near 10, 11 and 23.8 km s^{-1} which disappeared at some epochs then reappeared at other ones. The features at 10 and 11 km s^{-1} were observed from 1984 May to 1990 September, while the feature at 23.8 km s^{-1} was seen only from 1988 November to 1989 April (Fig. A3). Analysis done below (Sect. 3.4, Fig. 14) clearly indicates that the bursts of emission near 10 and 11 km s^{-1} largely contribute to the integrated flux density. Similarly the appearance of a feature centred at 23.8 km s^{-1} resulted in an OH maximum of the red-shifted integrated emission. We note, that other OH maxima were not related to the bursts of individual features. The velocity extent of both maser lines of RT Vir indicates that they arise from a common envelope. Weak 1665 MHz emission at velocities of erratic 1667 MHz features shows a quite regular variability.

Summarising, we notice that the 1665 and 1667 MHz OH maser profiles of the studied semiregulars strongly deviate from the standard double-peaked profiles. It appears that changes in the 1667 MHz profiles due to bursts of individual features, tend to be more frequent than in the 1665 MHz profiles.

3.3. Flaring features

Maser features with eruptive variability were identified in RT Vir and W Hya. Variations of the linewidth at half maximum ΔV and peak flux density S_p of most interesting features at 1667 MHz during selected outbursts are plotted in Fig. 11. From 1985 May to 1987 July ($1374 \leq JD_m \leq 2031$) the feature centred at 8.8 km s^{-1} from RT Vir underwent peculiar changes; S_p decrease was associated with ΔV re-broadening at $1462 \leq JD_m \leq 1551$ (circles in Fig. 11a), while in the interval $1604 \leq JD_m \leq 1817$ S_p rise was associated with ΔV narrowing (squares in Fig. 11a). Although the presence of each effect relied on four points spanning 89 and 213 days, we believe that these were real. In the same source a re-broadening of the feature centred at 10 km s^{-1} was seen at $1574 \leq JD_m \leq 1667$ (circles in Fig. 11b). It is worth noticing that variations of S_p of both features were uncorrelated before $JD_m = 1817$. Furthermore, narrowing of the feature of W Hya centred

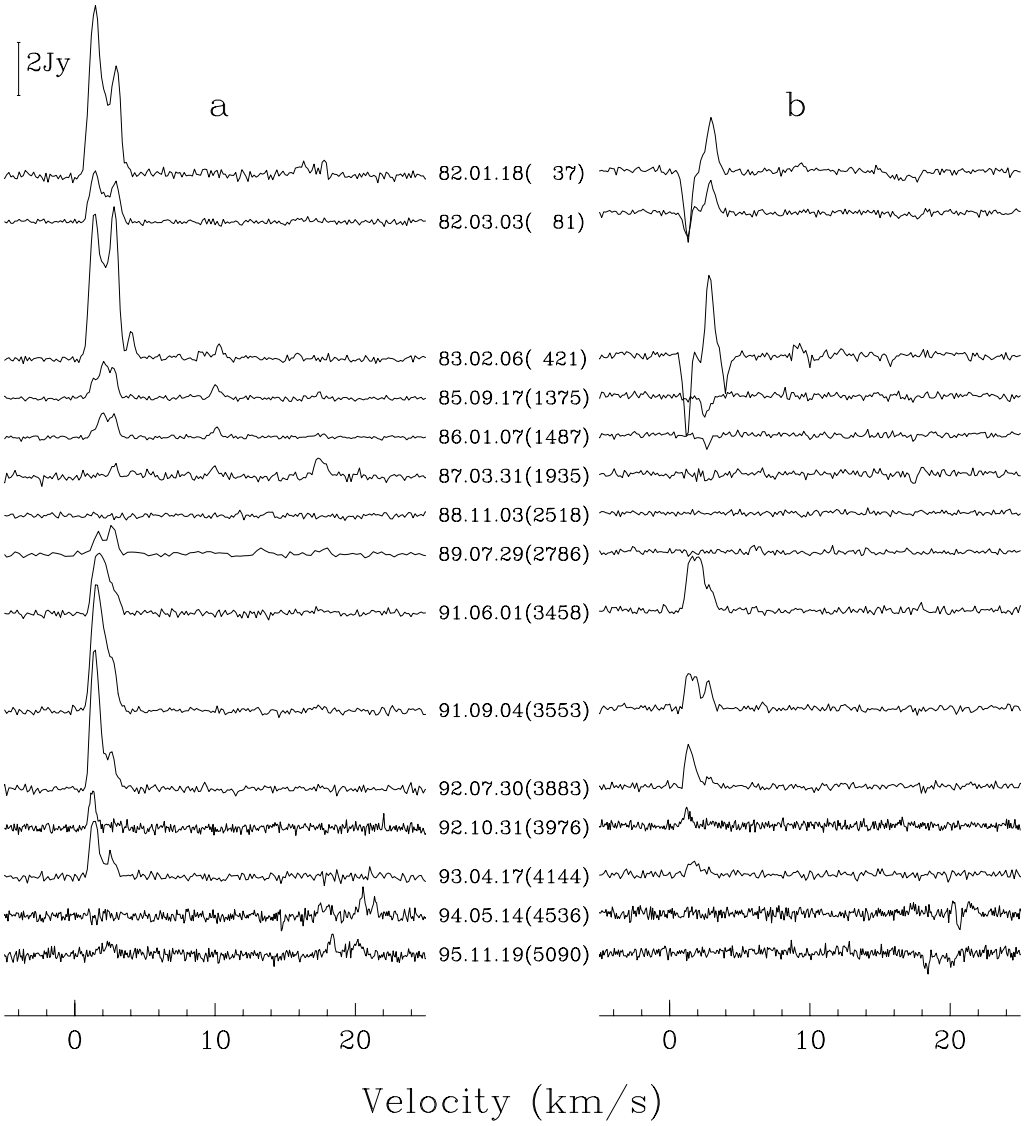

Fig. 2. Same as Fig. 1, but for the OH 1665 MHz maser emission.

at 46.5 km s^{-1} was visible at $4899 \leq \mathrm{JD_m} \leq 4935$ (squares in Fig. 11c).

We found an inverse relationship between the linewidths and peak flux densities which followed a power law $\Delta V \sim S_{\mathrm{p}}^{-\alpha}$ with $0.19 < \alpha < 0.57$. Two possibilities can be considered to explain this effect. The line narrowing and re-broadening may result from blending of spectral features which are close in velocity. A blending effect possibly occurs for OH masers from W Hya where the red-shifted emission is composed of several spectral features. Interferometric observations (Szymczak et al. 1998) support this supposition. However, the OH maser spectra of RT Vir are much simpler than those of W Hya and the effect of blending is probably too weak to mimic the line narrowing and re-broadening. The second possibility is that variations of the linewidth against peak flux are intrinsic to the OH emission. Such power law variations with $\alpha = 0.5$ are expected for unsaturated masers (Goldreich & Kwan 1974). Different values of α inferred for RT Vir possibly reflect a maser gain which changed in time from one maser feature to another. Uncorrelated variations of the peak fluxes in two spectral features of RT Vir strongly support this possibility. We conclude that bursts of OH emission from RT Vir with rise and/or decay times observed to be 90−200 days come from regions of different unsaturated maser gains.

3.4. OH variation curves

Figure 12 shows the integrated total fluxes (S_{int}) from R Crt at 1667 and 1665 MHz for the red-shifted, central and blue-shifted complexes. OH maser behaviour was similar at both frequencies. However, there was a general trend that the integrated flux of the blue-shifted emission was high when that of the red-shifted emission was weak. The behaviour of the OH emission at central velocities (7−16 km s^{-1}) was roughly similar to that at blue-shifted velocities. OH variability curves of R Crt presented high amplitude rises and declines of about 600−1200$^{\mathrm{d}}$ duration superimposed with shorter 550−610$^{\mathrm{d}}$ cyclic variations of smaller amplitude. During these last three cycles since 1990 September to 1995 November, when the radio data were better sampled, a modulation of the integrated

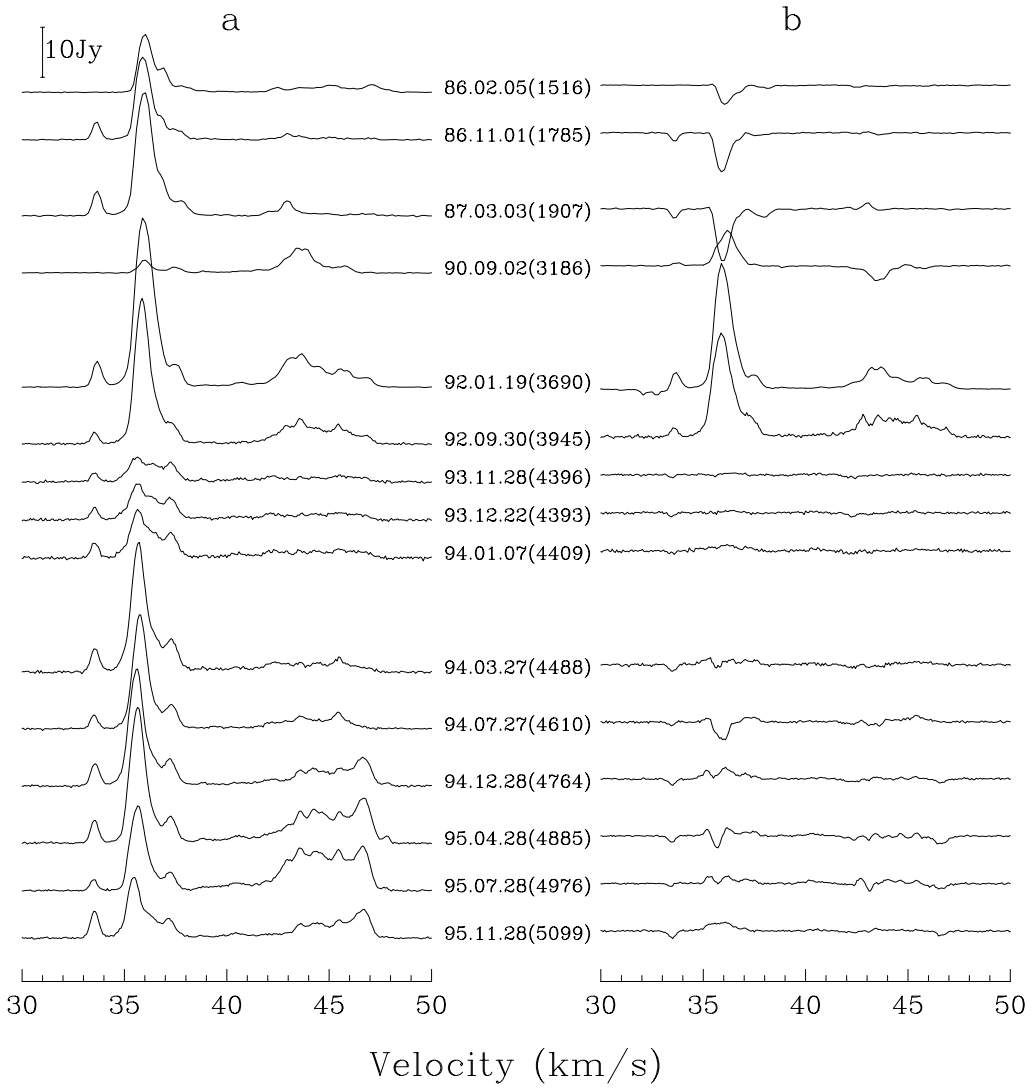

Fig. 3. Selected spectra of the OH 1667 MHz maser emission from W Hya in **a)** Stokes I and **b)** Stokes V taken from 1986 January to 1995 November. The flux density scale is shown by the vertical bar. JD_m dates are given in parentheses.

flux density with periods of about $160-200^d$ was apparent. Optical data available from AAVSO[1] AFOEV[2] and VSOLJ[3] were rudimentary, so that a detailed comparison with our data is not warranted. However, the optical brightness of R Crt may have been lower during the two last years of our OH observations (Fig. 12a). Furthermore, the weak $160-200^d$ modulations seen in the OH integrated flux density can correspond to the optical period of 160^d reported by Kholopov et al. (1985). We have used the most sampled parts of the OH variability curves (i.e., since 1990 September) for period analysis with the periodogram technique (Lomb 1976; Scargle 1982). With that technique, we found the two periodicities detected visually in the OH maser emission of R Crt (i.e., 560 ± 15^d and 227 ± 8^d, Table 2). The non-sinusoidal shape of the variability curves and large changes in amplitude from one cycle to other are probably the reason why the probability of a 160^d period was below 95%.

The integrated OH maser fluxes of W Hya showed considerable variations, sometimes by about an order of magnitude during less than 600^d, in both mainlines (Fig. 13). The behaviour of the blue-shifted and red-shifted emissions was roughly similar in both lines over the whole interval of observations. The 1667 MHz emission at central velocities generally followed the changes of the red-shifted emission but with more moderate amplitude. The variations of the central velocity emission at 1665 MHz were small. Good sampling of data from 1993 November to 1995 December allowed us to identify two consecutive maxima of small and large amplitudes with a period of 380^d. Furthermore, secondary maxima were seen in the 1667 MHz red-shifted emission, while at 1665 MHz shorter variations with a period of about 200^d were evident. The periodogram analysis of these observations revealed periodicities of 362 ± 7^d at both OH maser frequencies (Table 2). The main OH period of 362^d agrees very well

[1] American Association of Variable Star Observers.
[2] Association Française des Observateurs d'Étoiles Variables.
[3] Variable Star Observers League in Japan.

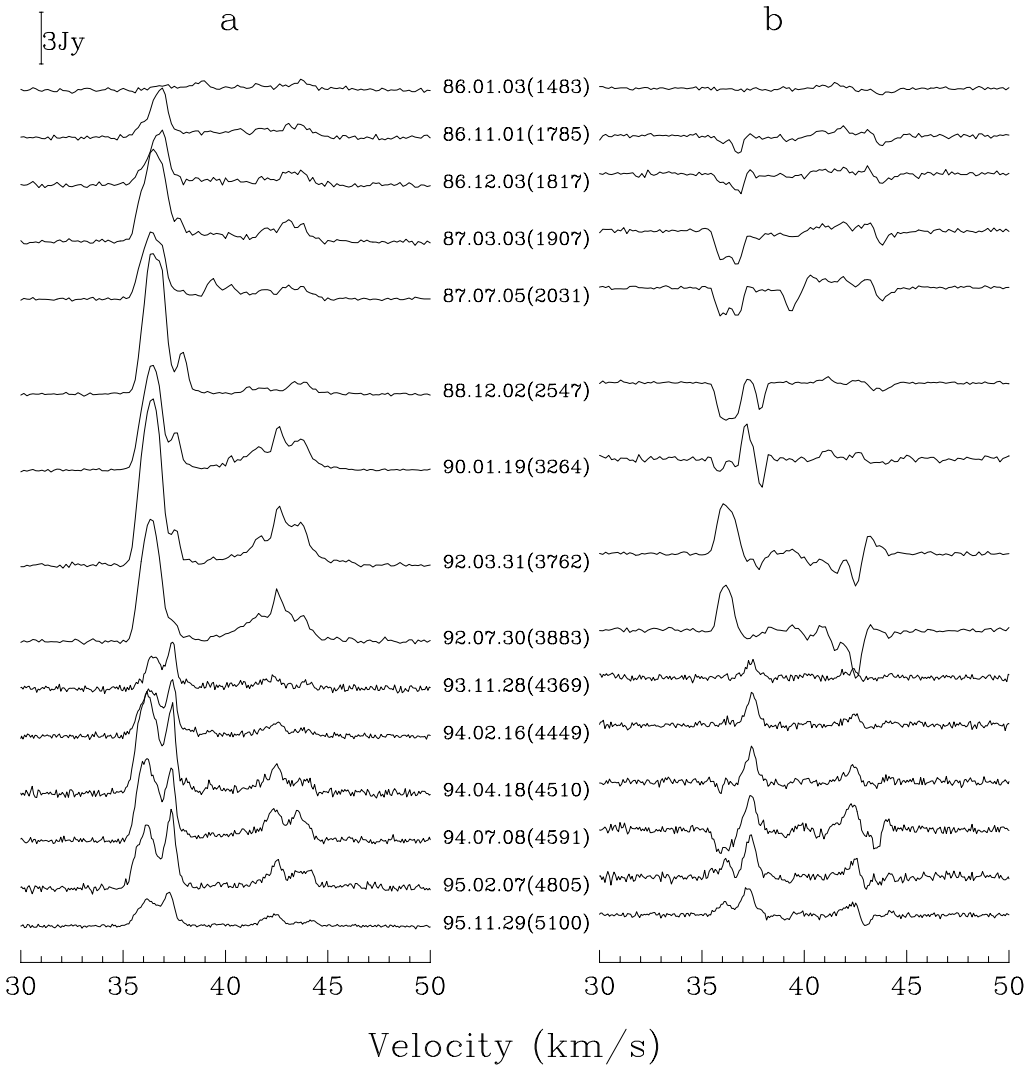

Fig. 4. Same as Fig. 3, but for the OH 1665 MHz maser emission.

with the average, optical period (Kholopov et al. 1985). On the average the OH maxima were delayed by $16 \pm 10^{\mathrm{d}}$ with respect to the optical maxima deduced from VSOLJ and AFOEV data. The phase lag (i.e., the time shift) between the OH 1667 MHz flux curves in the red-shifted and blue-shifted emission was $20 \pm 13^{\mathrm{d}}$. This corresponds a shell of radius 9.0–42.6 $\times\ 10^{15}$ cm. We note that this lower limit was a factor of two higher than the average radius measured with MERLIN (Szymczak et al. 1998). This suggests that in the case of W Hya the lower limits of the phase lag measurements should be considered as roughly consistent with the interferometric data. We observed a delay of $64 \pm 14^{\mathrm{d}}$ between the OH 1667 MHz flux density maxima of the extremely blue-shifted peak at 33.8 km s^{-1} and the standard blue-shifted peak at 36 km s^{-1}. This implies that the extreme blue-shifted emission, unresolved with MERLIN (Szymczak et al. 1998), arises at a distance of about 2.9×10^{16} cm from the central star (see Sect 4.1).

The OH variability curves of RT Vir are shown in Fig. 14. The variations of the red-shifted and blue-shifted parts of the spectra in both OH mainline were generally independent. Rises and decays of the OH flux by a factor of 3–6 during 120–140 days and low amplitude changes lasting a few thousand days were observed. Weak 1665 MHz emission close to the stellar velocity was sporadically present. Over the best sampled part of the integrated flux curves (1993 November–1995 November) we found a $170 \pm 7^{\mathrm{d}}$ periodicity in the 1667 MHz red-shifted emission. Furthermore, a shorter cycle of $112 \pm 11^{\mathrm{d}}$ duration was observed in both mainlines. Their formal confidence limits were above 0.95. Those OH periods differ by 15–43$^{\mathrm{d}}$ from the optical period of 155$^{\mathrm{d}}$ quoted by Kholopov et al. (1985). The optical data from the

Table 2. Variability periods of the studied semiregulars.

Star	Optical period[1] (days)	OH periods (days)
R Crt	160	227 ± 8; 560 ± 15
W Hya	360	362 ± 7
RT Vir	155	112 ± 11; 170 ± 7

[1] From Kholopov et al. (1985).

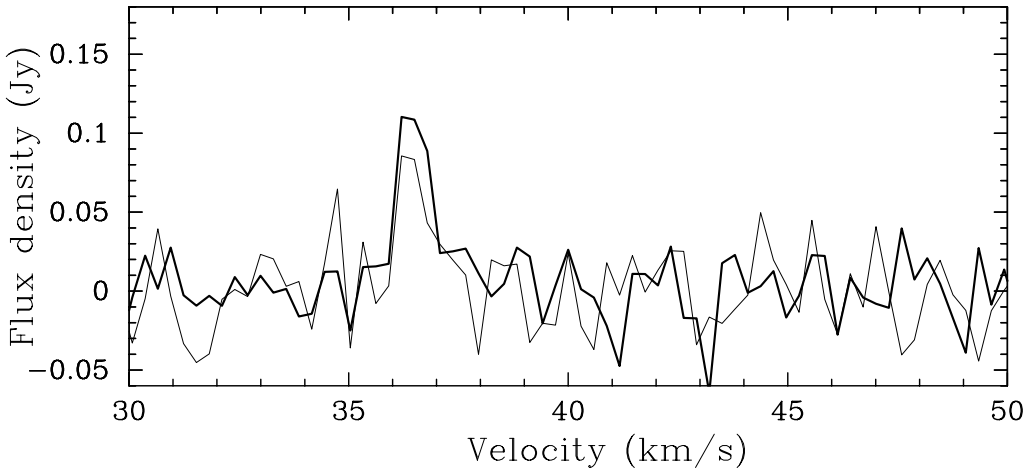

Fig. 5. Spectrum in the 1612 MHz maser line from W Hya discovered around the OH mainline maximum of August 23−26, 1990. The spectrum presented is the average of 3 hours of observation. Thick and thin lines represent RHC and LHC polarisations respectively.

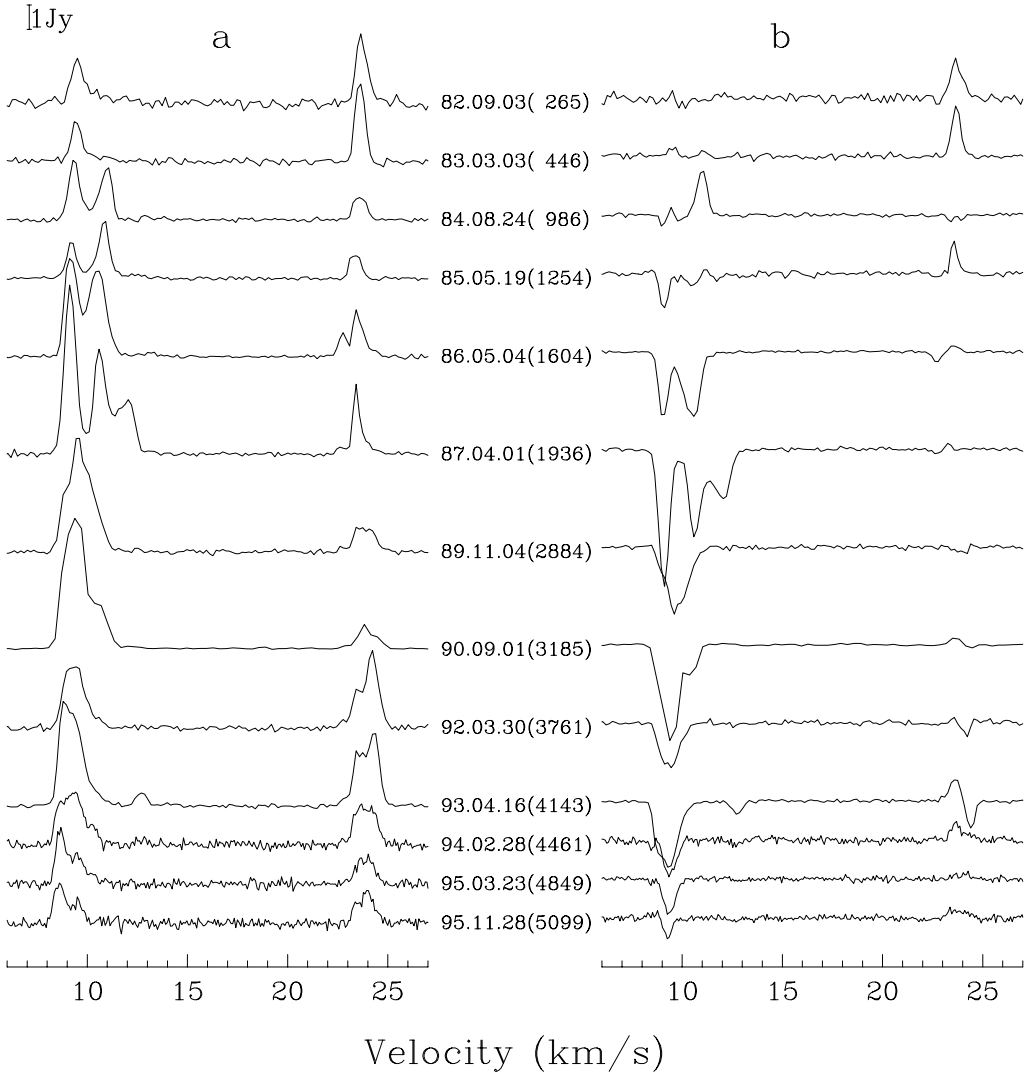

Fig. 6. Selected spectra of the OH 1667 MHz maser emission from RT Vir in **a)** Stokes I and **b)** Stokes V taken from 1982 April to 1995 November. The flux density scale is shown by the vertical bar. JD_m dates are given in parentheses.

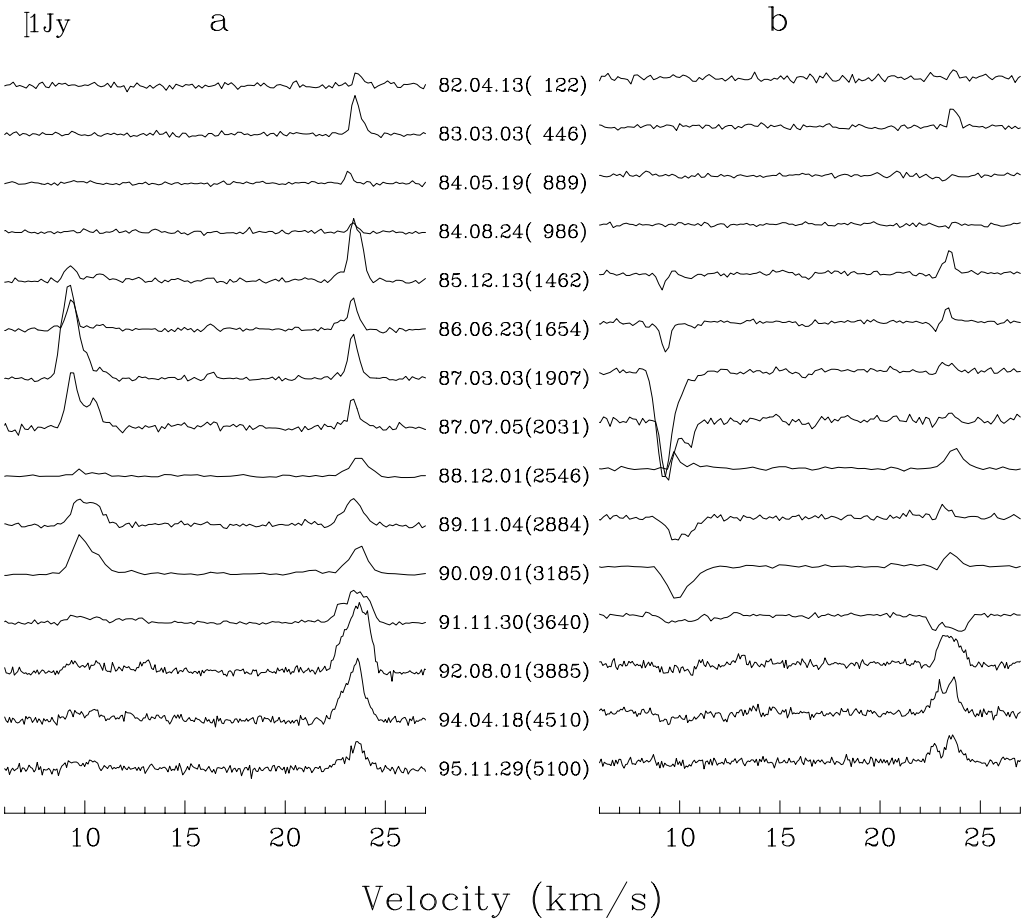

Fig. 7. Same as Fig. 6, but for the OH 1665 MHz maser emission.

Table 3. Amplitudes (Δm) of OH variations between consecutive minima and maxima in the three semiregulars. In parentheses are given the amplitudes over the entire intervals of observations.

Source	1665 MHz				1667 MHz			
	blue		red		blue		red	
R Crt	0.92−2.45	(5.3)	0.81−1.85	(4.7)	1.05−2.41	(6.2)	1.01−1.41	(2.0)
W Hya	0.34−2.44	(5.0)	0.92−3.97	(3.8)	0.60−3.68	(3.8)	0.52−1.68	(3.1)
RT Vir	0.42−2.42	(3.9)	0.75−2.30	(2.7)	0.57−0.71	(2.9)	0.34−2.08	(2.1)

interval of our observations are too incomplete to look for any relation with the radio variations.

In order to quantify better the OH variability curves we measured the amplitude between a consecutive maximum and minimum of the total integrated flux densities defined as $\Delta m = 2.5\log(S_{\rm int}(\max)/S_{\rm int}(\min))$. The ranges of amplitudes measured in both mainlines for the blue-shifted and red-shifted emissions of the 3 semiregular stars are given in Table 3. We note that the ranges of OH amplitudes of the studied semiregulars (0.3−4.0) are similar to that observed for Miras (Etoka & Le Squeren 2000). Amplitudes of $S_{\rm int}$, also measured in magnitudes, over the entire intervals of observations, given in parentheses in Table 3, range from 2.0 to 6.2 which are comparable to those values reported for some Miras (Etoka & Le Squeren 2000). In all three stars these amplitudes are higher for blue-shifted emission than for red-shifted emission for both mainlines. In general, Δm is higher at 1665 MHz than at 1667 MHz. This suggests, at least for W Hya, that the variability decreases with the radial distance of the maser envelope from the star.

3.5. Line ratio

The ratios of the integrated flux density at 1667 MHz to that at 1665 MHz for both the blue-shifted and red-shifted emission for the 3 sources are presented Fig. 15. For the blue-shifted emission of R Crt, this ratio was about 2 during most observing epochs. At $3400 < {\rm JD_m} < 3800$ only this ratio was as high as 6−10. This ratio for the red-shifted emission of R Crt was about 2 at the following $\rm JD_m$ intervals: 0–400, 3200–4200 and 4350–4440, while

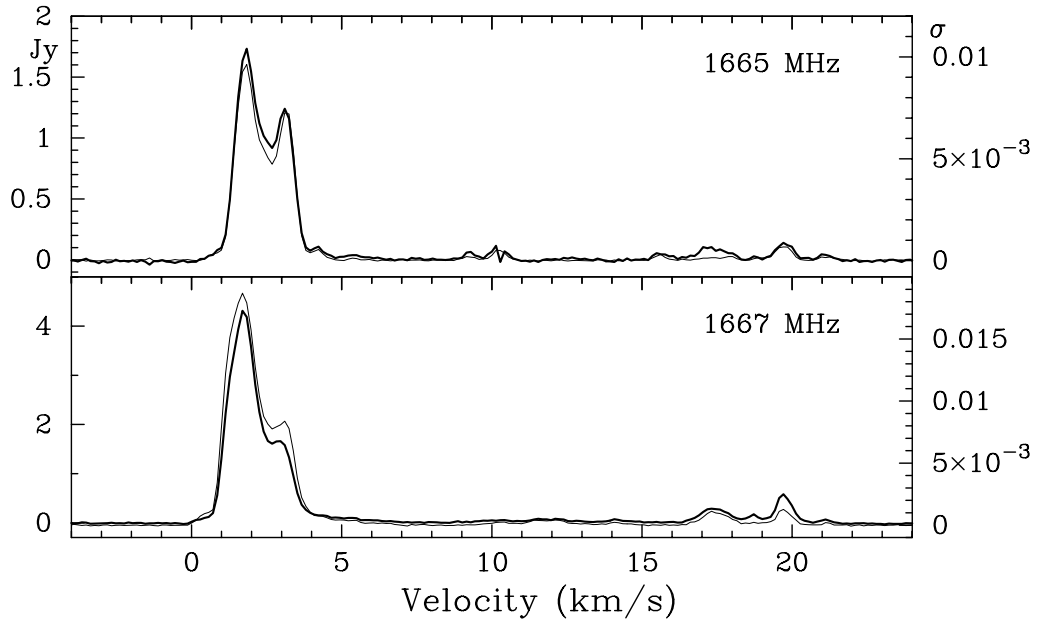

Fig. 8. The average OH maser line profiles (thick lines and left axis) and the variability index across the profiles (thin lines and right ordinate axis) for R Crt.

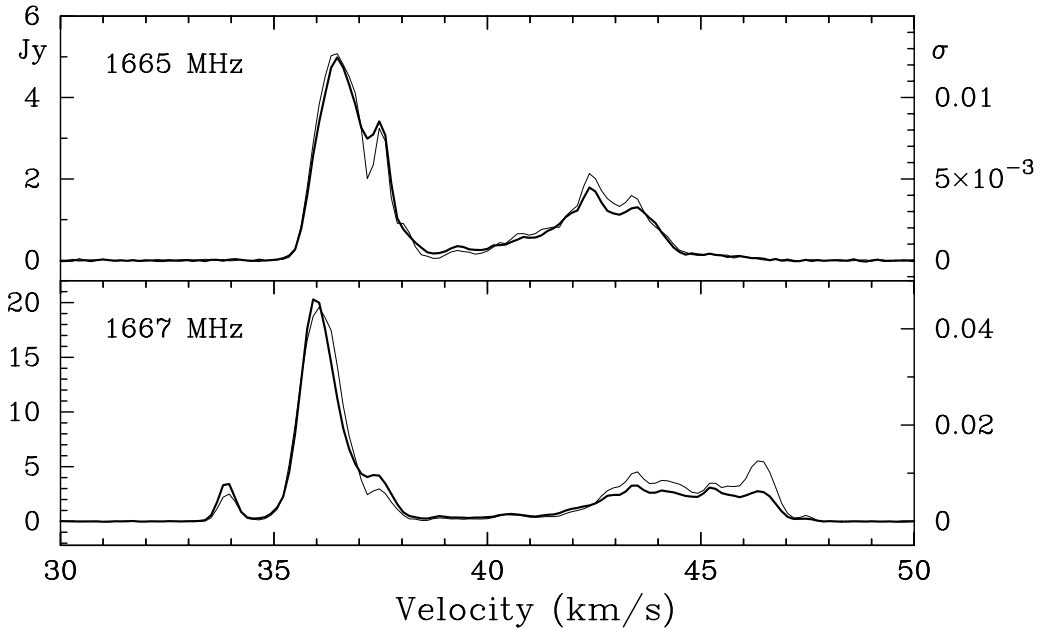

Fig. 9. Same as Fig. 8, but for W Hya.

during other epochs it varied from 4 to 14. In W Hya and RT Vir the ratio was generally about 2 for the blue-shifted emission and rarely higher than 4. In turn, for the red-shifted emission of either source the ratio was typically above 4 and could exceed 20. In all three sources we found a trend for the ratio to be about 2 during epochs of high OH activity, reaching its highest values during periods of low level maser emission. The line ratio value is suggested to be a function of the fractional abundance of OH molecule (Collison & Nedoluha 1994); an envelope of lower fractional abundance has dominant 1667 MHz emission. It is likely that during a period of quiet OH emission the fractional abundance of OH decreases and 1667 MHz emission becomes dominant. Our results seem to support the suggestion of Collison & Nedoluha.

4. Discussion

4.1. Periodicities and detached shells

Cyclic variations in the OH mainline emission were found for the three semiregular variables. The OH period

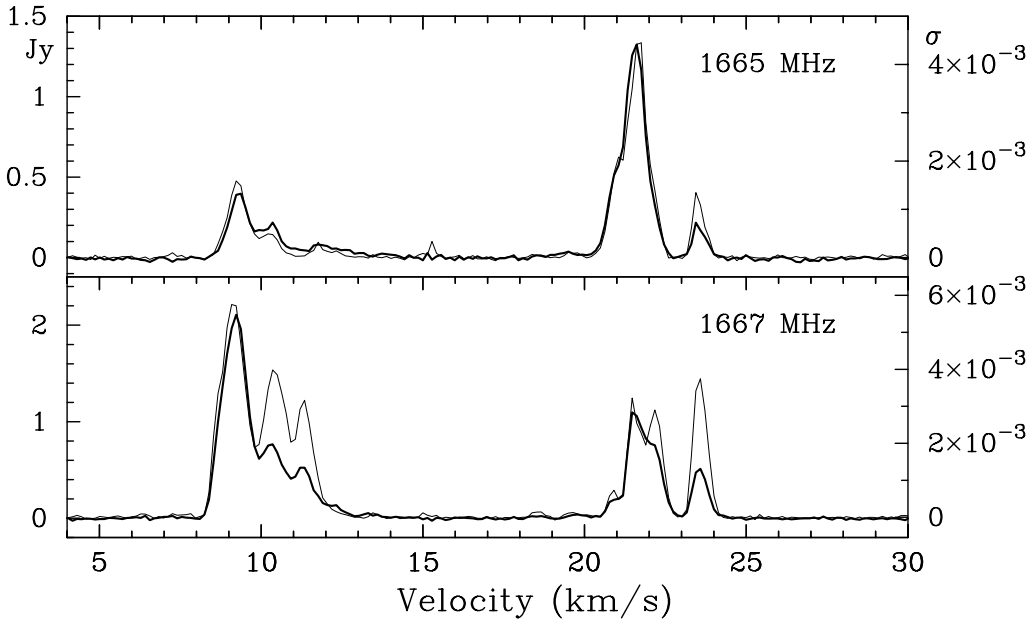

Fig. 10. Same as Fig. 8, but for RT Vir.

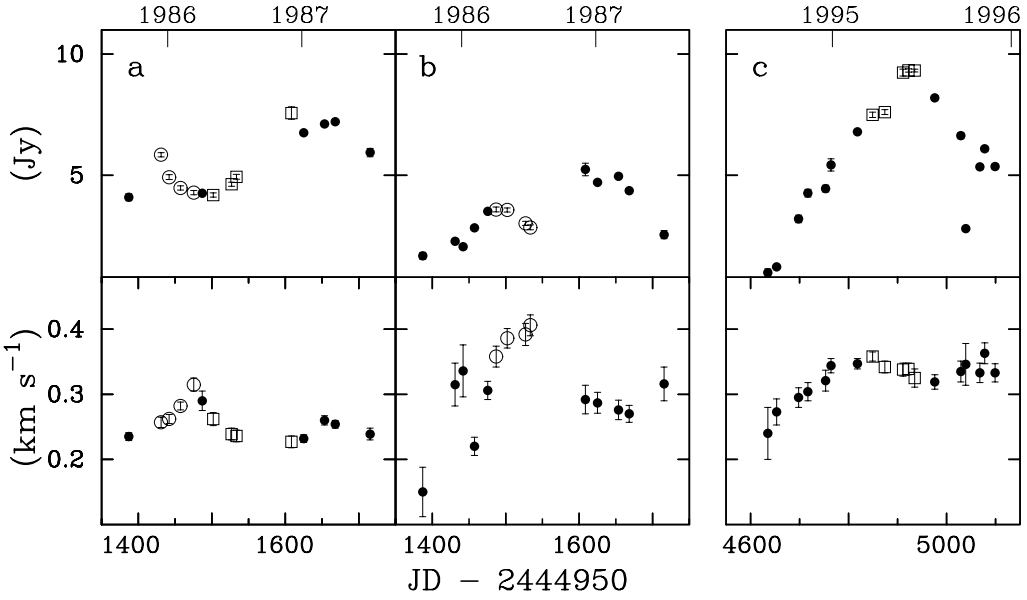

Fig. 11. Variations of the peak flux density (upper panels) and linewidth (lower panels) for the 1667 MHz features of RT Vir at 8.8 km s^{-1} **a)** and 10 km s^{-1} **b)**, and of W Hya at 46.5 km s^{-1} **c)**. Circles and squares denote the observing intervals of line re-broadening and narrowing respectively.

inferred for W Hya, which is classified as SRa star, agrees very well with the optical period (Kholopov et al. 1985). In contrast, both SRb stars, R Crt and RT Vir have two OH periods (determined from the most sampled intervals of data) which differ from the optical periods given by Kholopov et al. (1985). This discrepancy is likely to be due to the scarcity of the optical data for both objects, but multi-periodic variations of OH masers can also have non-trivial causes. We note sub-cycles in the variability of all three stars. These resemble the bumps usually observed in the optical and OH variability curves of classical Miras (Etoka 1996; Etoka & Le Squeren 2000) but these are more prominent in the semiregulars. The bumps and the long-term variations over several cycles may be related to the dust formation mechanism. Winters et al. (1994) have shown that, taking into account the dynamic structure of the dust shell, secondary maxima are produced in light curves at wavelengths longer than 2.2 μm as an effect of the thermal emission contribution of newly formed dust layers in the most inner part of the circumstellar shell.

As noted in Sect. 3.2, emission from W Hya near 46.5 km s^{-1} is transient but can be bright. We suggest this comes from the red-shifted parts of a detached shell, the blue-shifted parts of which possibly produce the emission

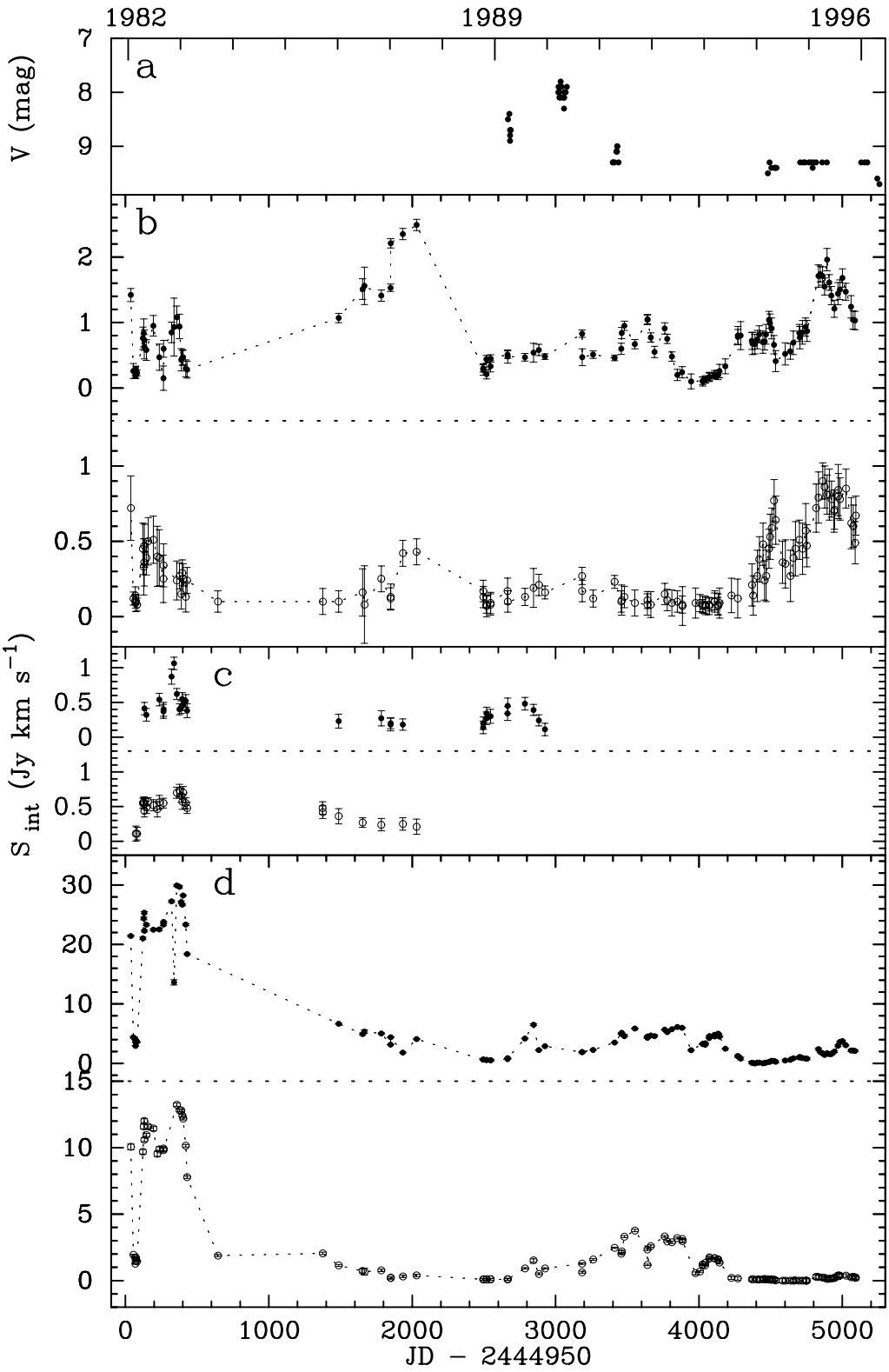

Fig. 12. Variability curves of R Crt. Optical data from AFOEV and VSOLJ **a)**, the integrated flux densities (Stokes parameter I) at 1667 MHz (filled circles) and 1665 MHz (open circles) for the blue-shifted **b)**, central **c)** and red-shifted **d)** emissions.

near 33.8 km s^{-1}. Phase-lag measurements (Sect. 3.4) indicate that this feature arises at a greater distance from the star than the rest of the blue-shifted OH mainline emission but which is typical for 1612 MHz emission. Such detached shells could result from the super-periodicities in dust formation predicted by Winters et al. (1994).

Gómez Balboa & Lépine (1986) studied the integrated flux variations of the 22 GHz maser emission of late-type

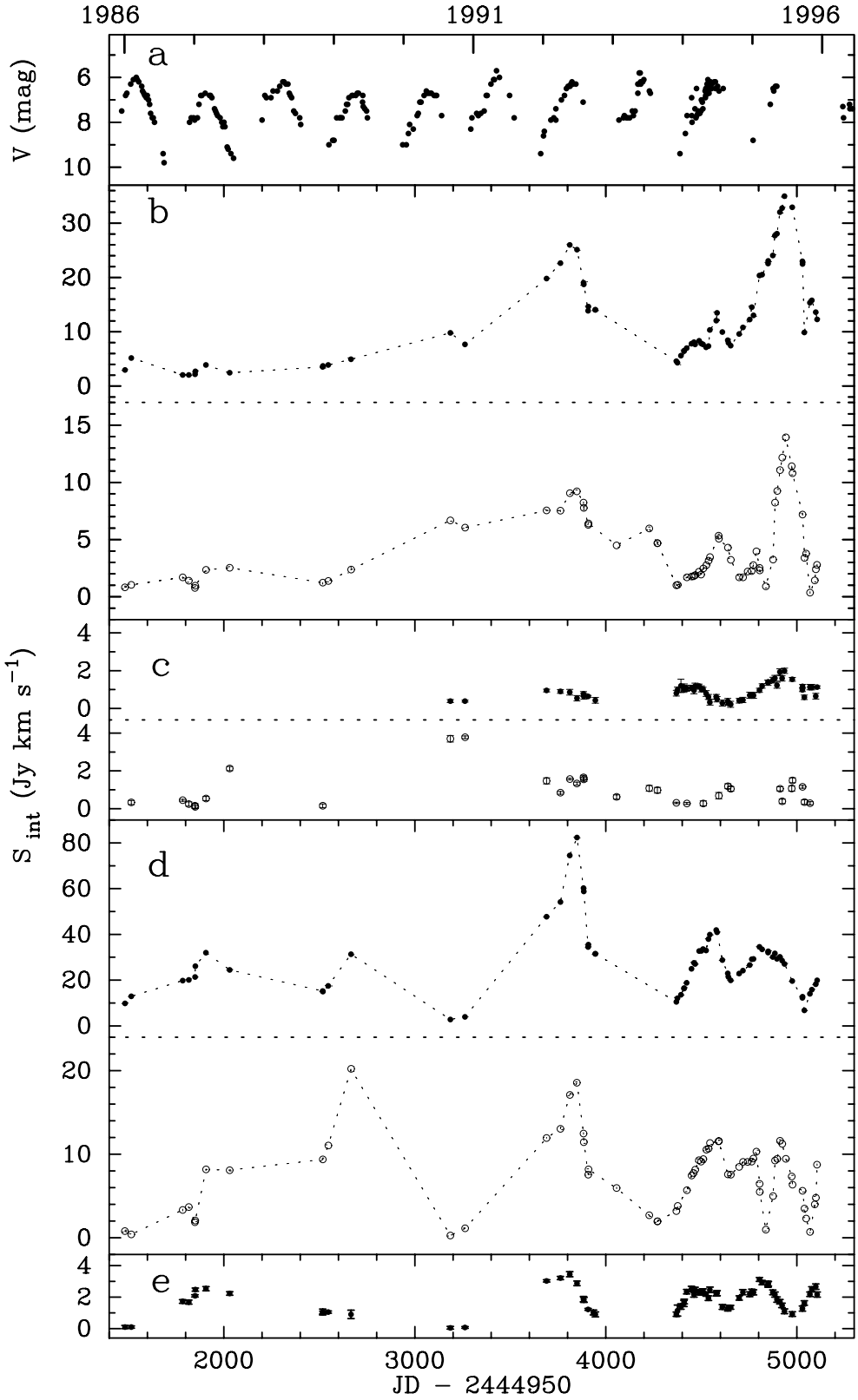

Fig. 13. Same as in Fig. 12, but for W Hya. Variations of the integrated flux densities of the extreme blue-shifted emission near 33.8 km s^{-1} **e)** are shown.

stars including R Crt and W Hya from 1976 August to 1982 February. They observed aperiodic variations in the H_2O maser emission of R Crt which span several cycles. W Hya showed super-periodic behaviour on timescales which were multiples of the fundamental period. We note

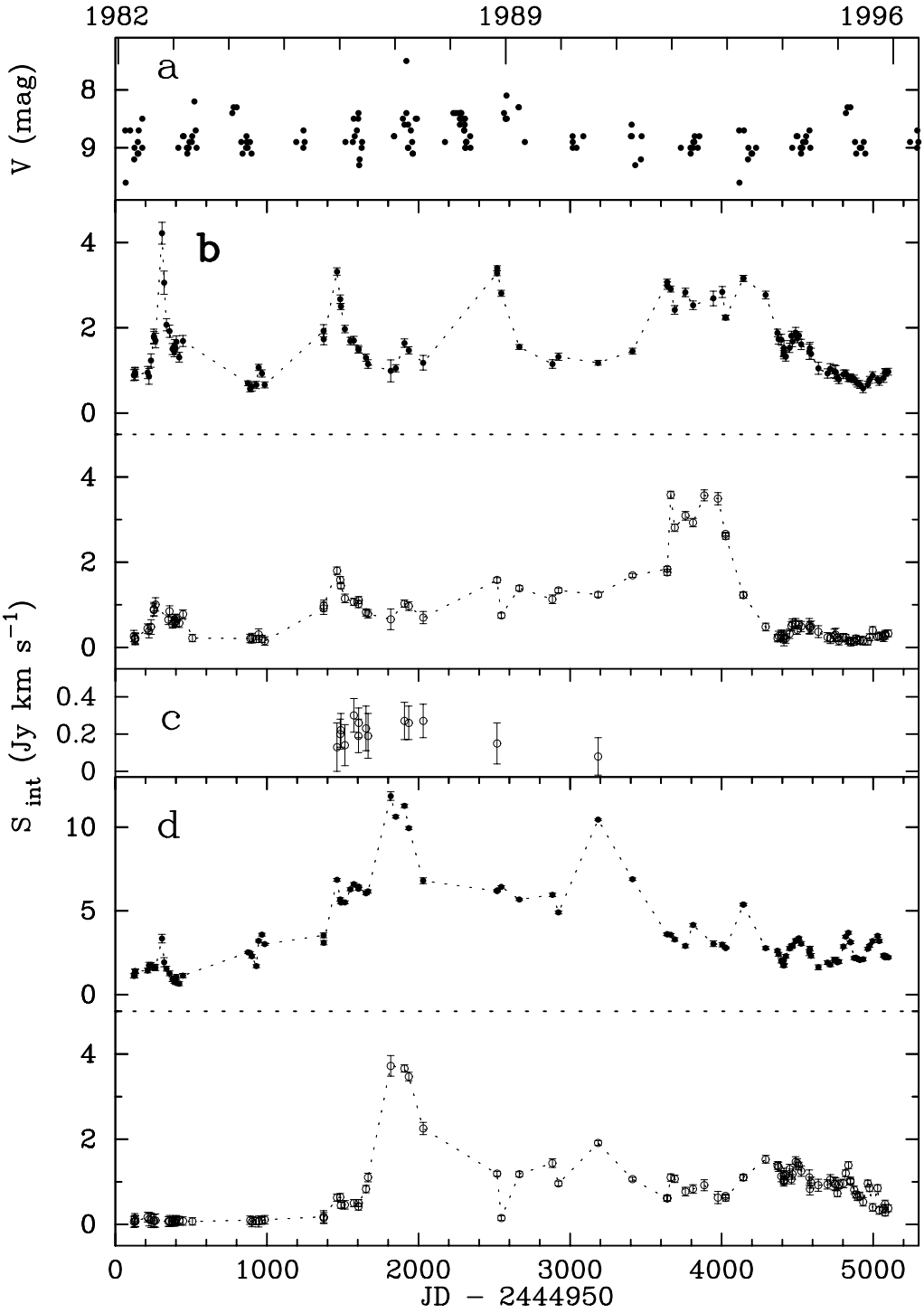

Fig. 14. Same as in Fig. 12, but for RT Vir.

that OH maser behaviour observed by us is quite similar to that reported for the water masers.

4.2. Peculiar behaviour

In contrast to the long term behaviour of the integrated flux of Miras (Etoka 1996; Etoka & Le Squeren 2000), variations in the integrated OH flux density of the semiregulars are quite large, up to a factor 10 during less than 600 days. Erratic behaviour of the OH mainlines is expected from theoretical calculations as an effect of transient instabilities in hotter and less dense regions of the envelope with low optical depth (Elitzur 1978). We documented well a few features which exhibit a flaring behaviour. The relationship between their linewidths and peak flux densities suggests that unsaturated amplification operate in some clouds of the OH envelope. This possibility is strongly supported by temporal variations of

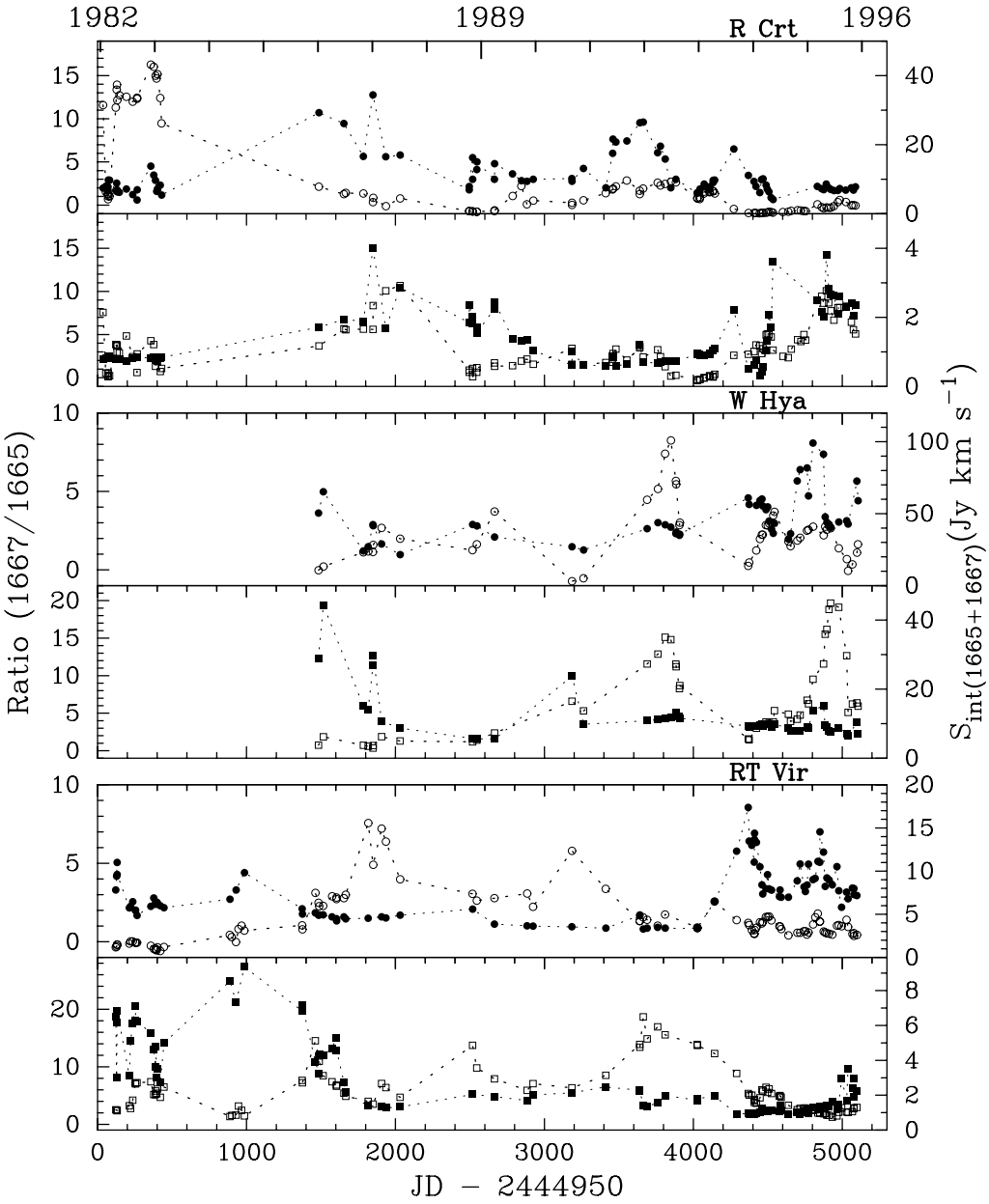

Fig. 15. Ratio of the integrated flux density at 1667 MHz over that at 1665 MHz (filled symbols) and the integrated flux density summed over both mainline transitions (open symbols) as a function of time for the three semiregular variables. For each source the blue- and red-shifted emission is shown separately in upper and lower panels, respectively.

their peak fluxes uncorrelated with the total intensities. There are other examples of such behaviour, but with our spectral resolution we cannot be sure whether an effect of line narrowing or re-broadening is mimicked by blending. Observations at higher spectral resolution and high angular resolution should be useful to eliminate possible blending of features.

The appearance of a very blue-shifted feature at 1667 MHz in W Hya, which makes the profile deviate from a standard double-peaked shape, possibly reflects a global change in excitation conditions of the maser envelope. This outermost feature is likely to emerge from an old OH envelope possibly excited by the central source as observed at 1667 MHz in U Her (Sivagnanam et al. 1989). Detection of faint emission at 1612 MHz from the same source is consistent with the view that in the outer parts of the maser envelope, favourable conditions just occurred. No 1612 MHz emission was detected towards R Crt and RT Vir, which is certainly due to a thinner circumstellar shell for these SRb stars. This is consistent with the interferometric data (Szymczak et al. 1999) for R Crt.

4.3. Tangential amplification

Although the OH profiles of the studied semiregulars are far from classical, most of the OH emission appears to be

beamed along radial paths. Weak emission at velocities very close to the systemic velocity occurred during some time intervals in R Crt and RT Vir, and almost always in W Hya as an effect of tangential beaming. In R Crt and RT Vir, the appearance of tangential emission usually coincides with a high level of total OH emission. In W Hya, the 1667 MHz emission at the systemic velocity usually follows the total emission, while the 1665 MHz emission is random and less stable than the radial emission. We note that the tangential emission of the OH semiregulars occurs preferentially during the periods of high maser activity in the envelopes. Tangential beaming requires a maser shell of sufficient width, or at least containing clumps of sufficient sizes to supply sufficient column densities for maser amplification.

In December 1995 an interferometric observation of R Crt with a high angular resolution was made (Szymczak et al. 1999) and the brightest peaks at 1665 and 1667 MHz had brightness temperatures greated than 3×10^6 and 5×10^6 K, respectively. No tangential emission was detected during that observation. Fortunately, at both mainlines during $1650 < \mathrm{JD_m} < 1850$ when tangential emission was present, the level of radial emission was the same as during interferometric measurements. In extrapolating the above brightness temperatures to that epoch some useful information can be inferred from the observed properties of tangential radiation. At the epoch considered, the peak flux ratios of the tangential to the radial emission were 0.16 and 0.04 at 1665 and 1667 MHz, respectively. Assuming that tangential emission does not come from a complete ring-like structure but rather from a single cloud, those ratios allow to evaluate the brightness temperatures of tangential emission in both mainlines. This assumption about the structure of the tangential emission is well supported by the simple unblended shape of the feature identified as tangential emission for both R Crt and RT Vir. There is also another well known source VX Sgr in which OH emission near the systemic velocity comes from a single cloud (Szymczak & Cohen 1997). However this does not appear to be the case for W Hya as OH emission at close v_s is obviously blended and may come from extended structures of low emission which is below the sensitivity limit of modern instruments. For R Crt the brightness temperatures deduced for tangential emission are greater than 5×10^5 and 2×10^5 K at 1665 and 1667 MHz respectively. The standard model of maser amplification (Goldreich & Kwan 1974) predicts that corresponding optical depths τ are -13.1 and -12.2. As the linewidth of the maser feature narrows by a factor $\sqrt{-\tau}$, then the observed linewidths of 0.24 and 0.26 km s^{-1}, at 1665 and 1667 MHz respectively, correspond to the thermal linewidths at half maximum Δv of 0.87 and 0.91 km s^{-1}. These imply a kinetic temperature in the regions of tangential emission of 290−320 K. R Crt has an OH envelope of radius $R_\mathrm{OH} = 9 \times 10^{14}$ cm (Szymczak et al. 1999), therefore with an expansion velocity of $v_\mathrm{e} = 9$ km s^{-1}, the gain length of the tangential maser is $R_\mathrm{OH}\Delta v/v_\mathrm{e} = 9 \times 10^{13}$ cm. The lower limit of linewidth of tangential maser emission is about 0.18−0.20 km s^{-1}. This suggests that when the kinetic temperature drops below 150−200 K, tangential amplification is not longer maintained in the envelope of R Crt. We believe that the gas temperature is an important factor which can influence the tangential amplification at distance below 10^{15} cm from the star.

4.4. Evolutionary status of OH semiregulars

Kerschbaum & Hron (1992) deduced that SRa stars are a mixture of "intrinsic Miras" and SRb stars, this latest group has been divided into two groups: the "blue" semiregulars with no indication of circumstellar shell and for which optical periods are lower than 150 days and effective temperatures are greater than 3200 K, and the "red" semiregulars with similar effective temperatures and mass loss rates as Miras but with a period about half as long. Jura & Kleinmann (1992) have inferred similar conclusions. In their classification, W Hya belongs to their first group of semiregulars with optical periods of 300–400 days and is a member of "thin disk" population of Miras. R Crt and RT Vir with optical periods ranging from 150 to 200 days belong to the third group of semiregulars according to classification scheme of Jura & Kleinmann. This group may have more than one main progenitor population. On the other hand, the mass loss rates of the studied OH semiregulars are about 10^{-7} $M_\odot$ yr^{-1} (Kahane & Jura 1994; Loup et al. 1993). This is only slightly lower than those derived for OH Miras (Sivagnanam et al. 1989). Our data support the view that W Hya belongs to Mira population showing OH behaviour different from that of the two SRb stars. The observed bursts and less regular variations of the OH emission of the two SRb stars imply that they have thinner OH envelope than W Hya as a result of recent lower mass loss rates. The OH periodicity (longer than 250 days) determined from our data for R Crt and W Hya together with the OH expansion velocities (7−11 km s^{-1}) well obey the period − OH velocity relation established for Mira and OH/IR (Sivagnanam et al. 1989). This suggests that W Hya is as evolved as Miras. Two SRb stars may be either in a Mira-like stage or post-Mira.

5. Conclusions

We have monitored the OH maser emission of three semiregular variables with the Nançay radio telescope over intervals spanning 10−14 years. This study leads to the following conclusions:

1. The OH masers show cyclic variations with slow high amplitude ($4-6^\mathrm{m}$) rises and declines, superimposed with fast low amplitude ($0.3-2^\mathrm{m}$) changes. The OH curves of W Hya follow optical variations, which is expected for radiative pumping. The variations of the OH masers from R Crt and RT Vir are less regular and the inferred radio periods are inconsistent with the optical periods. Erratic behaviour of these OH masers can be due to transient instabilities in hotter thinner envelopes. Well-sampled

optical data will be important to check a possible radiative coupling of the OH mainline masers with the stellar variability.

2. There is evidence for the presence of an outer detached OH shell around W Hya with a radius of over 10^{16} cm. Emission at 1667 MHz at extreme velocities appears erratically, and its variability profile compared with other parts of the shell and with interferometric observations suggests it is at distances typical of a 1612 MHz shell. Emission at this frequency has been detected once only. OH emission from the outer shell appears to sporadically excited at times of general high OH activity.

3. All studied stars sometimes show a weak emission near the systemic velocity which is due to tangential amplification. This emission usually appears during a high level of the total OH emission which is predominantly radially beamed. For R Crt, we found that the tangential emission decreased below our sensitivity limit when the kinetic temperature in the maser envelope drops below 150–200 K.

4. We observed bursts of the 1667 MHz features in RT Vir and W Hya. The line narrowing and re-broadening on timescales of 90–200 days are well documented for 3 features. The inverse relationship between the linewidth and the peak flux density established for those features suggests variations in the maser gain during unsaturated amplification.

5. The ratios of the flux density at 1667 MHz over that at 1665 MHz in all the three stars were about 2 at epochs of high OH activity and usually increased during weak maser emission. This finding seems to support the theoretical prediction that the line ratio is a function of the fractional abundance of OH molecules.

6. Simultaneous single dish and interferometric observations at high angular resolution of these and other maser transitions which probe different circumstellar regions and regular optical observations would provide useful data to extend our findings.

Acknowledgements. We would like to thank Anita Richards for helpful suggestions on the manuscript. S. E. thanks the "Société de Secours des Amis des Sciences" for financial support through a research grant. The Unité Scientifique Nançay of the Observatoire de Paris is associated as Unité de Service et de Recherche USR No. B704 to the French Centre National de Recherche Scientifique (CNRS).

References

Collison, A. J., & Nedoluha, G. E. 1993, ApJ, 413, 735
Collison, A. J., & Nedoluha, G. E. 1994, ApJ, 422, 193
Dickinson, D. F., Bechis, K. P., & Barrett, A. H. 1973, ApJ, 180, 831
Elitzur, M. 1978, A&A, 62, 305
Etoka, S. 1996, Ph.D. Thesis, Université de Paris VI
Etoka, S., & Le Squeren, A. M. 1996, A&A, 315, 134
Etoka, S., & Le Squeren, A. M. 1997, A&A, 321, 877
Etoka, S., & Le Squeren, A. M. 2000, A&AS, 146, 179
Fillit, R., Proust, D., & Lépine, J. R. D. 1977, A&A, 58, 281
Goldreich, P., & Kwan, J. 1974, ApJ, 190, 27
Gómez Balboa, A. M., & Lépine, J. R. D. 1986, A&A, 159, 166
Harvey, P. M., Bechis, K. P., Wilson, W. J., & Ball, J. A. 1974, ApJS, 27, 331
Jewell, P. R., Elitzur, M., Webber, J. C., & Snyder, L. E. 1979, ApJS, 41, 191
Jura, M., & Kleinmann, S. G. 1992, ApJS, 83, 329
Kahane, C., & Jura, M. 1994, A&A, 290, 183
Kerschbaum, F., & Hron, J. 1992, A&A, 263, 97
Kholopov, P. N., et al. 1985–88, General Catalogue of Variable Stars, 4th ed. (Nauka Publishing House, Moscow)
Le Squeren, A. M., & Sivagnanam, P. 1985, A&A, 152, 85
Lomb, N. R. 1976, Ap&SS, 39, 447
Loup, C., Forveille, T., Omont, A., & Paul, J. F. 1993, A&AS, 99, 291
Neufeld, D., Chen, W., Melnick, G., et al. 1996, A&A, 315, 237
Palen, S., & Fix, J. D. 2000, ApJ, 531, 391
Sivagnanam, P., Le Squeren, A. M., Foy, F., & Tran Minh, F. 1989, A&A, 211, 341
Scargle, J. D. 1982, ApJ, 263, 835
Szymczak, M., & Cohen, R. J. 1997, MNRAS, 288, 945
Szymczak, M., Cohen, R. J., & Richards, A. M. S. 1998, MNRAS, 297, 1151
Szymczak, M., Cohen, R. J., & Richards, A. M. S. 1999, MNRAS, 304, 877
Szymczak, M., Le Squeren, A. M., Sivagnanam, P., Tran-Minh, F., & Fournier, A. 1995, A&A, 297, 494
Wallerstein, G., & Dominy, J. 1988, ApJ, 326, 292
Winters, J. M., Fleisched, A. J., Gauger, A., & Seldmayr, E. 1994, A&A, 290, 623
Young, K., Phillips, T. G., & Knapp, G. R. 1993, ApJ, 409, 725